IEEE Access
Multidisciplinary | Rapid Review | Open Access Journal

Received December 11, 2020, accepted December 22, 2020, date of publication December 25, 2020,
date of current version January 12, 2021.

Digital Object Identifier 10.1109/ACCESS.2020.3047514

3D Printed Al_2O_3 for Terahertz Technology

JAN ORNIK[1], MASOUD SAKAKI[2], MARTIN KOCH[1], JAN C. BALZER[3], AND NIELS BENSON[2], (Member, IEEE)

[1]Department of Physics and Material Sciences Center, Philipps-University Marburg, 35032 Marburg, Germany
[2]Faculty of Engineering, Institute of Technology for Nanostructures, University of Duisburg-Essen, 47057 Duisburg, Germany
[3]Chair of Communication Systems, University of Duisburg-Essen, 47057 Duisburg, Germany

Corresponding authors: Jan Ornik (jan.ornik@physik.uni-marburg.de) and Niels Benson (niels.benson@uni-due.de)

This work was supported by the German Research Foundation within the C13 Project of the SFB/TRR 196 MARIE.

ABSTRACT In this work we demonstrate that 3D printed Al_2O_3 is a promising material for prototyping and precise fabrication of quasi-optical devices in the terahertz frequency range. The 3D printed Al_2O_3 exhibits a low absorption coefficient ($\alpha < 2\text{cm}^{-1}$at 1 THz) and a high refractive index ($n > 3$). The printing resolution in the sub 50 μm range allows for the implementation of structures in the 0.3-3.0 THz range on the subwavelength scale. Furthermore, the printing process enables the realization of crystalline solids, which allows the use of the Al_2O_3 birefringence effect. Here, a $\Delta n \approx 0.05$ was achieved and used for the implementation of $\lambda/2$-wave plates working at $\sim$1 THz. The material properties and wave plates were characterized using a terahertz time-domain spectrometer.

INDEX TERMS 3D printing, ceramics, Al_2O_3, terahertz, wave plate.

I. INTRODUCTION

During the last twenty years, terahertz (THz) technology has made tremendous progress. Now, on the one hand THz systems are used for basic research in labs worldwide [1]–[3] and on the other hand many practical applications are foreseen for THz technology. These applications are predominantly in the fields of non-destructive material and structural testing [4]–[6], as well as sensing [7]–[9]. Further, short-range wireless communication is expected to become a mass market in a few years from now [10]–[12]. Consequently, THz sources and THz detectors were further developed in recent years and a multitude of passive devices to guide or manipulate THz waves have been demonstrated. This includes filters [13], reflectors [14], lenses [15], diffraction gratings [16], waveguides [17] and couplers [18], beam splitters [19] and last, but not least wave plates [20], [21].

A promising way for fast prototyping and fabrication of THz devices is 3D printing (additive manufacturing) [15], [17], [18], [22]–[25]. The main advantage of 3D printing is the monolithic fabrication of complex structures at low cost, high accuracy and high fabrication speed for small volume production [26]. 3D printing of different polymers and their applications in the THz range have been studied by various researchers [15], [18], [23], [24], [27]–[29]. Until now, most demonstrations of 3D printed THz devices are restricted to fused deposition modeling (FDM) manufacturing. The two main limitations for this technology is the poor resolution of more than 100 μm and the limited availability of highly transparent printable polymers [30]. Further, all highly transparent polymers have a refractive index on the order of 1.5, which prevents the fabrication of ultra-thin devices as well as photonic crystals with large bandgaps, where a large contrast in refractive index is beneficial. Further, material properties which can increase the functionality of the devices, such as birefringence are not known for FDM based 3D printed materials.

A material class which has the potential to overcome these challenges are ceramics. Compared to polymers, ceramics usually have a higher refractive index and some ceramics, such as Al_2O_3, show a low absorption coefficient at THz frequencies [31]–[33]. Furthermore, the crystalline form of Al_2O_3 also known as sapphire, is known to exhibit large birefringence in the THz range [34]. This could lead to birefringence of a 3D printed Al_2O_3 ceramic samples, if some degree of crystallinity is induced during the printing process. Therefore, the 3D printing of ceramics offers new possibilities for precise fabrication of low-loss and compact THz devices of complex shapes depending on the manufacturing method.

Various methods, including: SLS (Selective Laser Sintering), LOM (Laminated Object Manufacturing), IJP (InkJet Printing), Two-Photon Polymerization (TPP) and LCM (Lithography-based Ceramic Manufacturing), have been

The associate editor coordinating the review of this manuscript and approving it for publication was Norbert Herencsar.

invented for 3D printing of ceramics [35]. However, of these techniques, the LCM technology has the highest potential for THz applications, due to the combination of high material quality and a potential structural resolution in the sub 50 μm range. LCM utilizes ceramic particles suspended in a photocurable resins as the printing material (i.e. printing slurry). While printing layer by layer, polymerization of the suspension through controlled UV irradiation will form a green body, which consists of the polymerized polymer and ceramic particles, of the desired shape. After printing, the green body is debindered and subsequently sintered to form the final ceramic part [36]–[38]. The LCM method has been successfully employed for the fabrication of ceramic parts such as: turbine blades and gear wheels [37], as well as first mm and sub-mm wave applications such as wireless RFID (radio-frequency identification) tags [39]–[41].

In order to further establish ceramic additive manufacturing for mm and sub-mm wave applications, a quantification of the dielectric properties for 3D printed ceramics in the THz range is vital. However, to the best of our knowledge, these properties are currently unavailable for most of the 3D printed ceramic materials. Hence, the aim of the research discussed in the following has been the investigation of the dielectric properties for LCM Al_2O_3 in the frequency range between 0.3 and 2.5 THz. Here, we discuss Al_2O_3, as it is one of the most widely used ceramics [42]. Based on the observed birefringence phenomenon in the sample, we further demonstrate a $\lambda/2$ wave plate application in the THz range.

II. EXPERIMENTAL SECTION

A. 3D PRINTING OF Al_2O_3

Cylindrical Alumina samples were fabricated using the LCM method. For this purpose, a Lithoz CeraFab 7500 [43] printer was used with a X, Y and Z resolution of 40 μm, 40 μm and 50 μm, in combination with LithaLox HP350 [43] UV curable slurry containing 49 vol% of high purity Al_2O_3 ($\sim$ 99.8%).

During printing, layer by layer specific UV exposure (t: 4.4 s/layer, energy: 220 mJ/cm^2/layer) initiated the polymerization reactions in the slurry, and brought about the formation of the 3D green bodies. Fig. 1 a) shows the schematic image of a printed sample. It should be noted, that the sample was built perpendicular (i.e. standing on) on the building platform. This minimizes its contact area with the building platform and facilitates the device detachment after the completion of the printing step. Subsequently, the support structure was carefully removed and the sample was cleaned using a LithaSol 20 [43] cleaning fluid, in order to wash out the residue of the slurry (i.e. unpolymerized slurry).

Conversion of the green samples into the final parts was achieved using an electric furnace with the following temperature cycle programming: I) Preconditioning: T_{Max} = 120 °C, heating rate = 0.2 K/min, dwell time = 3 days, II) Debindering: T_{Max} = 1100 °C, heating rate = 1 K/min, dwell time = 5.8 days and III) Sintering: T_{Max} = 1700 °C, heating rate = 0.8 K/min, dwell time = 4.3 days. IV) Cooling: The furnace turned off and cooled naturally. In Fig. 1 images of a green and a sintered 3D printed sample are shown. It can be seen, that the sample has shrunk about 21 Vol% during the sintering step, mainly due to the polymer burn-out during the debindering step.

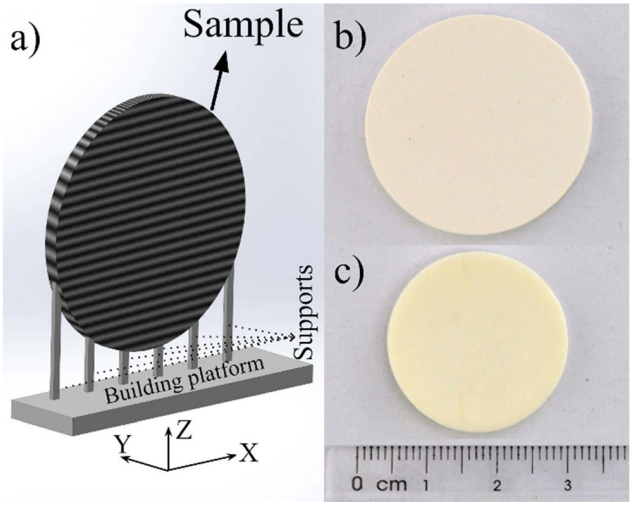

FIGURE 1. Schematic image of the a) printed sample as well as photographs of b) green and c) sintered Alumina.

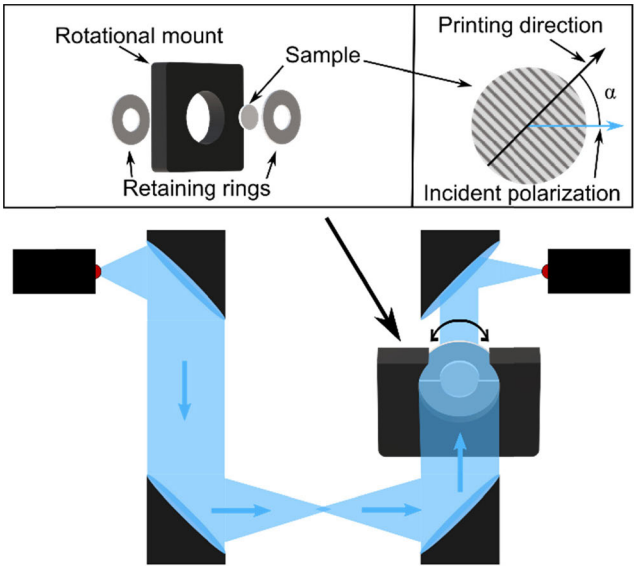

FIGURE 2. Sketch of the setup. The arrows indicate the propagation direction of the THz radiation. The inset shows how the sample was mounted into the rotational mount and defines the angle α between the printing direction and the polarization of the THz radiation incident on the sample. The retaining rigs with clear aperture of approximately 22 mm were covered with aluminum foil to block part of the THz beam.

B. SAMPLE CHARACTERIZATION

A THz time domain spectroscopy (TDS) system [44] with a pair of fiber-coupled photoconductive antennas was used for the characterization of the samples. Four off-axis parabolic mirrors (OAPM) were used to guide the THz beam from

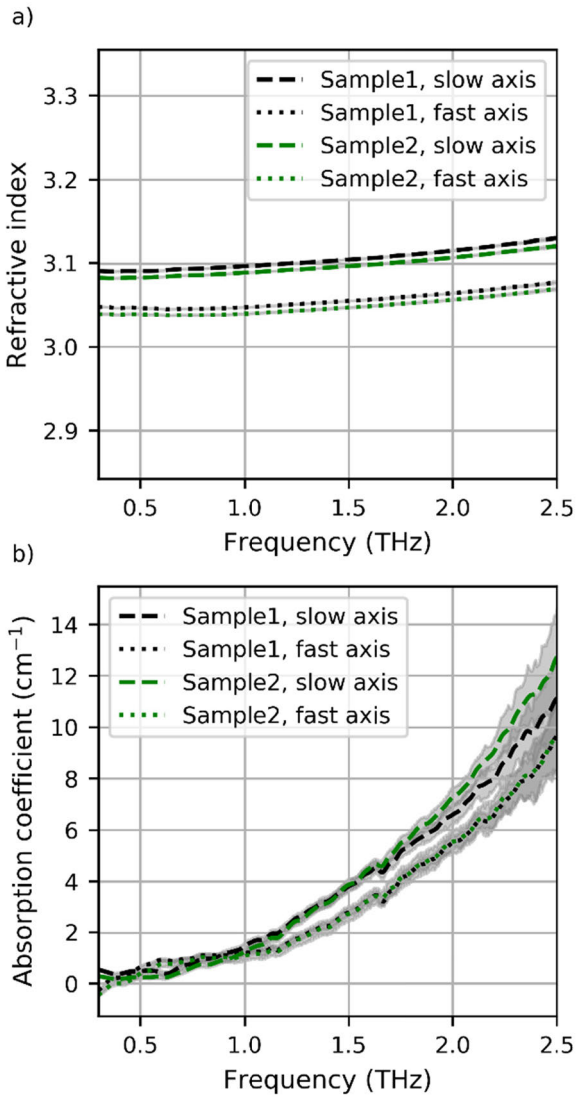

FIGURE 3. a) Refractive index and b) absorption coefficient of 3D printed Al_2O_3 along the fast and slow axis. The grey shaded area represents the measurement uncertainty due to the system instability. The corresponding time-domain and frequency-domain data as well as the imaginary part of the refractive index are available in the supplementary material.

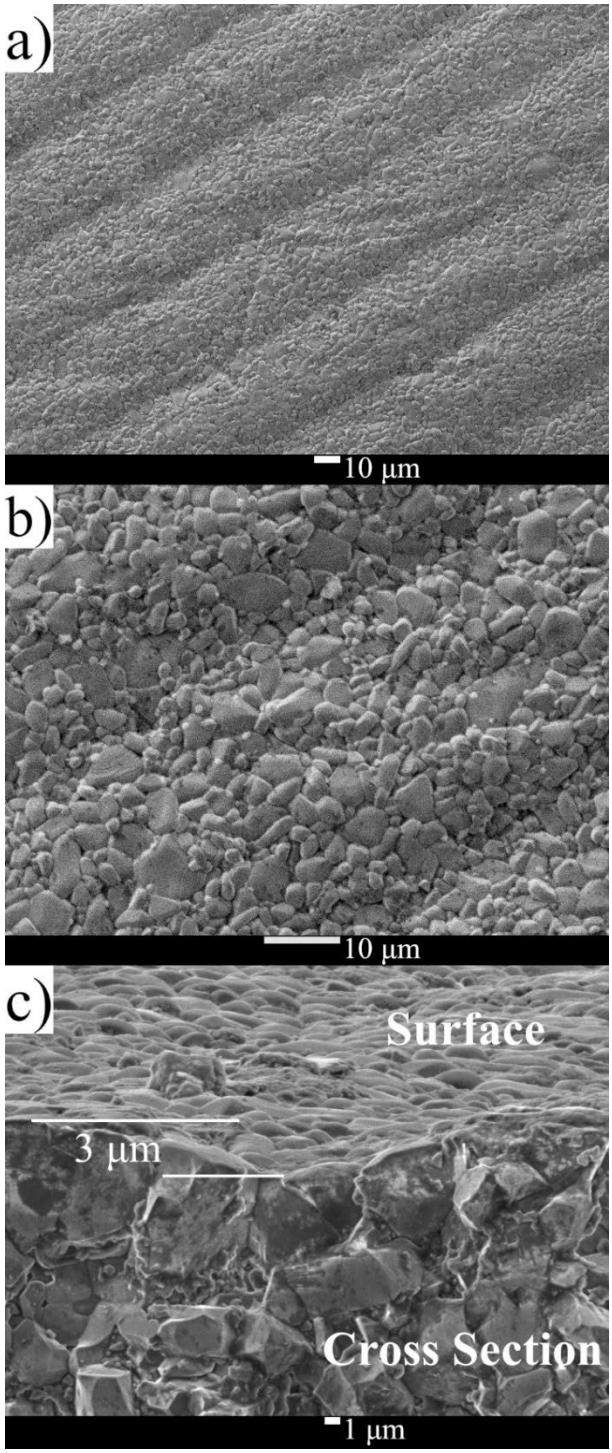

FIGURE 4. SEM images of the a) surface b) surface at higher magnification and c) the cross-section of 3D printed Al_2O_3 sample. The periodic surface structure resulting from the layer by layer additive manufacturing of the sample is approximately 3 μm thick.

the emitter antenna to the detector. Samples were inserted into a motorized rotational mount and placed between the last two OAPM before the detector, where the THz beam is collimated (Fig. 2). The reference measurements were taken with the rotational mount and retaining rings still in the beam path, however, without a sample in it. This was done, since the collimated beam size was greater than the sample size. During the measurements, the whole setup was flooded with nitrogen to minimize the absorption from water vapor present in the ambient air. The temperature in the lab was approximately 20.5 °C.

Preliminary investigation of the first sample revealed that the sample is birefringent and the approximate directions of the slow and the fast axes were marked. After a set of reference measurements, the sample was inserted into the rotational mount. The sample was orientated in such a way that at the initial position the two marked axes were either parallel or perpendicular to the polarization of the incident THz radiation. Then the sample was rotated for 360° in steps of 1° and for each angular step the sample transmission was

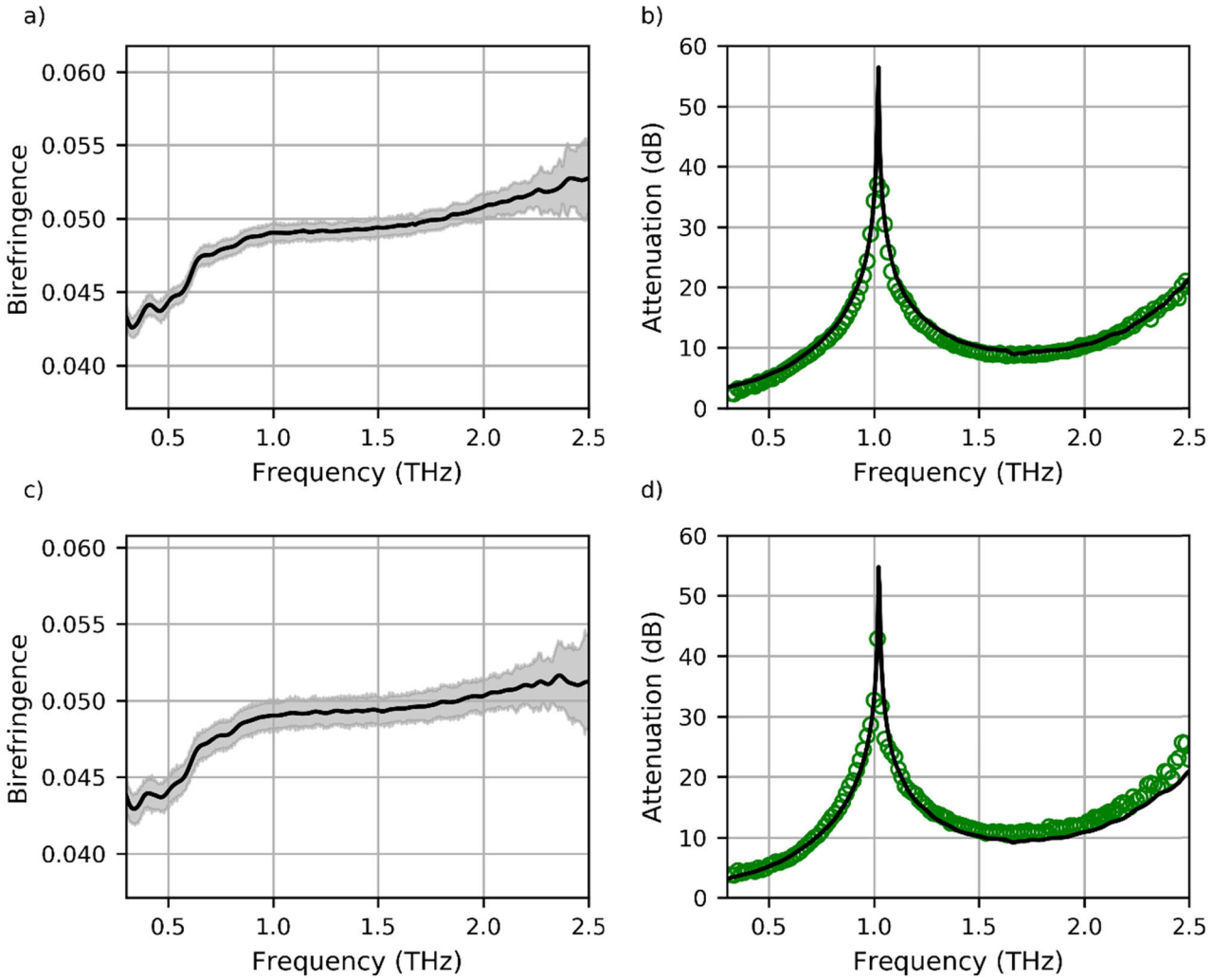

FIGURE 5. Samples 1 and 2 as $\lambda/2$ wave plate. a) measured birefringence and b) attenuation modeled and measured for sample 1 at $\alpha = 45°$. c) measured birefringence and d) attenuation modeled and measured for sample 2 at $\alpha = 45°$. The attenuation peak around 1 THz corresponds to the rotation of the polarization for 90° degrees due to the phase shift of π between the two polarization components. The green circles correspond to the measurement result and the black line to the modeled values.

recorded. With an analysis of these angular measurements, the orientation of the fast and slow axis was determined more precisely. Then the sample was remeasured ten times at orientations parallel to the two axes and directly afterwards ten reference measurements were performed. These data were used for the extraction of the refractive index and the absorption coefficient, which was performed using a commercially available software (Teralyzer).

The software is based on algorithms described in [45], [46]. For the evaluation of the refractive index and the absorption coefficient, the thickness of the sample needs to be determined, which was done in two steps. In the first step, the thickness of the samples was measured using a micrometer screw. This value was then used as a starting value in the second step, in which the Teralyzer software was used to further refine the thickness evaluation of the sample based on multiple-reflections of the THz radiation within the sample using the quasi-space approach [46]. The thickness determined in this way was used for both orientations of the sample (i.e. polarization parallel to the fast and the slow axis). The determined thickness was 3000 μm and 2990 μm for sample 1 and sample 2, respectively, which agrees well with the design thickness of 3000 μm.

As it will be discussed in the following section, the orientation of the two axes is related to the printing direction which could be determined from the residue of the printing supports (see Fig. 1 a)). Therefore, the second sample was mounted in such a way that the printing direction was approximately perpendicular to the polarization of the incident THz radiation. The measurements and extraction of refractive index and absorption coefficient were performed in the same way as for sample 1.

Following the THz TDS measurements, one of the Al_2O_3 samples was broken in half and its cross-sectional

microstructure as well as surface quality was evaluated using a Scanning Electron Microscope (SEM: JEOL JSM 7500F).

III. RESULTS AND DISCUSSION

Fig. 3 shows the refractive index and absorption coefficient along the fast and slow axis for both investigated samples. The grey shaded areas correspond to the measurement uncertainty due to the system instability, as calculated based on the ten repeated measurements.

For the case of sample 1, the refractive index increases with frequency from approximately 3.05 at 0.3 THz to 3.08 at 2.5 THz for the fast axis and from 3.09 at 0.3 THz to 3.13 at 2.5 THz for the slow axis. The same trend can be observed for sample 2, however, its refractive index was determined to be slightly lower compared to sample 1. This difference is attributed to the measurement uncertainty of the sample thickness, which is required for the parameter extraction from the measurement as described elsewhere [45], [46]. However, this sample thickness uncertainty does not influence the observed birefringence, since the same sample thickness was used when extracting the refractive index and the absorption coefficient for the slow and the fast axis of the same sample.

Both samples show low absorption coefficient values at lower frequencies ($\alpha < 2$ cm^{-1} at 1 THz). With increasing frequencies, however, the absorption coefficient also increases and exceeds 5 cm^{-1} at 2 THz. Minor differences between the determined absorption coefficient for the two samples can be observed, which are mainly within the measurement uncertainty as explained above. Yet, the diattenuation is mainly greater than the measurement uncertainty and can be observed for both investigated samples.

The determined values of the refractive index and absorption coefficient are in agreement with already reported values for ceramic Al_2O_3 [31]–[33]. However, the investigated 3D printed Al_2O_3 samples show birefringent properties, which is unusual for alumina samples. The direction of the slow and fast axis could be related to the printing direction (see Fig. 2), namely, the slow axis was found parallel to the printing direction and the fast axis perpendicular to it.

Illustrated in Fig. 4 are the results of an SEM study of our samples. Fig. 4 a) reveals a periodic surface structure, which is a consequence of the additive manufacturing layer by layer growth. Such periodic surface structures [47] as well as periodic layered samples [48] can cause a sample to be birefringent. However, in case of such a form birefringence, the slow axis would be perpendicular to the printing direction and the fast axis parallel to it, which is exactly the opposite to the measured birefringence. Therefore, this surface structure cannot be the reason for the observed birefringence. Furthermore, the expected birefringence from such a thin surface structure (~ 3 μm, see Fig. 4 c)), is more than an order of magnitude smaller compared to the observed one. Therefore, we suggest a different origin for the observed birefringence.

As the influence of stress birefringence also seems unlikely, we suggest this effect to be a consequence of sample

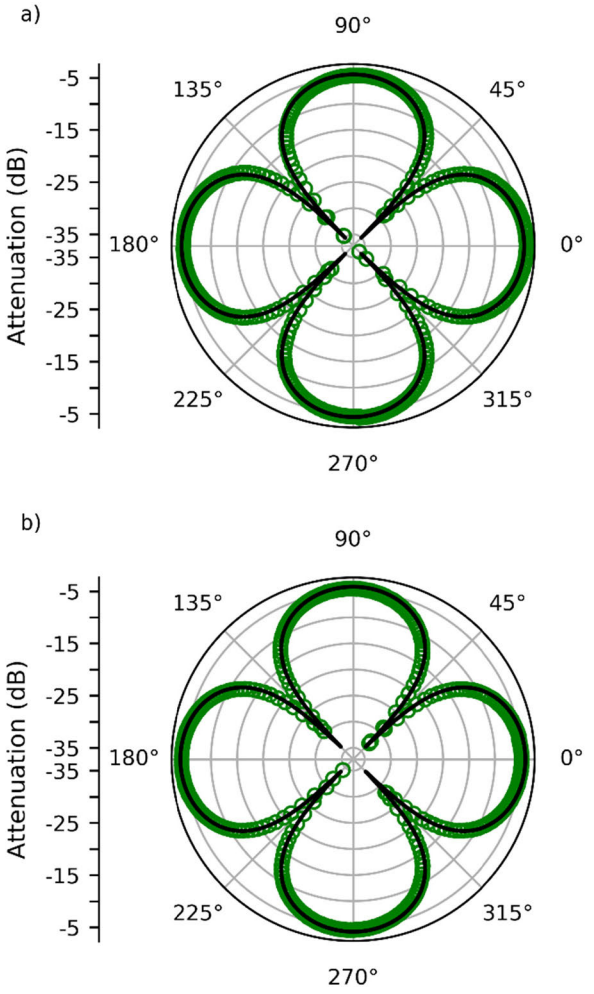

FIGURE 6. Angular dependent attenuation in the frequency range 0.98-1.04 THz for a) sample 1 and b) sample 2. The green circles correspond to the measurement result and the black line to the modeled values.

crystallinity with a preferred orientation. This may be the result of the layer by layer green body growth, as the orientation of the slow axis is parallel and the fast axis is perpendicular to the printing direction. We therefore hypothesize, that the printing and cross-linking mechanism results in a preferred crystallographic orientation, which manifests itself during the debindering and sintering step of the sample (Figure 4 b) and c)). As the printed samples are still polycrystalline, the observed birefringence of $\Delta n \approx 0.05$ is approximately a factor of 6 lower than the birefringence of Al_2O_3 single crystals ($\Delta n \approx 0.32$) as described by Kim *et al.* [34].

In the following, we use the birefringence effect of the printed Al_2O_3 ceramic to demonstrate a $\lambda/2$ wave plate as a first device made out of 3D printed Al_2O_3 working at approximately 1 THz.

Consider that THz radiation normally incidents on a sample with an angle α between the polarization of the incident electric field and the printing direction (slow axis) as depicted in Fig. 2. The incident electric field can be represented by two components, one parallel to the fast and the other to

the slow axis. If $\alpha = 45°$ then the two components are of equal amplitude. However, they propagate with a different phase velocity through the material, resulting in a phase shift between the two components. The phase shift can be calculated as

$$\Delta\varphi = 2\pi df\,\Delta n/c_0, \tag{1}$$

where Δn is the birefringence, f the frequency, d the plate thickness and c_0 the speed of light. If the phase shift equals π or its multiple and the diattenuation is small compared to the total attenuation, the initial polarization of the light is turned for 90° and the plate acts as a $\lambda/2$ wave plate. Considering that only polarization along the direction of the incident polarization is detected, the attenuation through such a sample can be modeled based on the Malus' law as [48]:

$$A = -10\log_{10}\left(T_{fast}T_{slow}\cos^2\left(\Delta\varphi/2\right)\right), \tag{2}$$

where T_{fast} and T_{slow} denote the transmittance for the individual electric field components. The birefringence of the two samples as well as the modeled and measured attenuation at $\alpha = 45°$ are shown in Fig. 5.

If a wave plate is placed under an angle different from $\alpha = 45°$, the components along the fast and slow axis are not of equal amplitude. In such a case, the polarization is turned for an angle different from 90° even if the phase shift is equal to π or its multiple. The angular dependent attenuation in the frequency range between 0.98 and 1.04 THz is shown in Fig. 6.

IV. CONCLUSION

In this contribution we report the refractive index and absorption coefficient values of 3D printed Al_2O_3 in a broad THz range from 0.3 THz up to 2.5 THz. The refractive index is found to be greater than 3 in this frequency range and the absorption coefficient to be lower than $2cm^{-1}$below 1 THz, which agrees with previous reports on ceramic Al_2O_3 [31]–[33]. Compared to polymers commonly used for 3D printing of THz devices, the 3D printed Al_2O_3 has significantly higher refractive index in this frequency range and a comparably low absorption coefficient with respect to the highly transparent polymers for frequencies lower than 1 THz [15], [27]. Furthermore, the investigated samples show birefringence ($\Delta n \approx 0.05$), which we attribute to a printing process dependent crystallinity of the LCM samples. As the birefringence of the 3D printed Al_2O_3 samples is related to the printing process, the birefringence might be tunable by adjusting the printing process parameters. Here we have employed the observed birefringence to demonstrate a $\lambda/2$ wave plate as a first device made out of 3D printed Al_2O_3 working at approximately 1 THz.

Consequently, the achieved material quality with the LCM technique in terms of a high refractive index ($n > 3$) and a low absorption coefficient ($\alpha < 2cm^{-1}$at 1 THz), in combination with high resolution digital 3D printing, opens a variety of possibilities for the implementation of complex structures and compact devices for the THz range. Exploring these possibilities as well as investigating the potential birefringence tunability of the 3D printed Al_2O_3 are part of ongoing research.

REFERENCES

[1] D. M. Mittleman, J. Cunningham, M. C. Nuss, and M. Geva, "Noncontact semiconductor wafer characterization with the terahertz Hall effect," *Appl. Phys. Lett.*, vol. 71, no. 1, pp. 16–18, Jul. 1997, doi: 10.1063/1.119456.

[2] T. Kampfrath, L. Perfetti, F. Schapper, C. Frischkorn, and M. Wolf, "Strongly coupled optical phonons in the ultrafast dynamics of the electronic energy and current relaxation in graphite," *Phys. Rev. Lett.*, vol. 95, no. 18, Oct. 2005, Art. no. 187403, doi: 10.1103/PhysRevLett.95.187403.

[3] F. R. G. Bagsican, M. Wais, N. Komatsu, W. Gao, L. W. Weber, K. Serita, H. Murakami, K. Held, F. A. Hegmann, M. Tonouchi, J. Kono, I. Kawayama, and M. Battiato, "Terahertz excitonics in carbon nanotubes: Exciton autoionization and multiplication," *Nano Lett.*, vol. 20, no. 5, pp. 3098–3105, May 2020, doi: 10.1021/acs.nanolett.9b05082.

[4] S. Hunsche, D. M. Mittleman, M. Koch, and M. C. Nuss, "New dimensions in T-ray imaging," *IEICE Trans. Electron.*, vol. E81-C, no. 2, pp. 269–275, Feb. 1998.

[5] T. Sasaki, T. Sakamoto, and M. Otsuka, "Sharp absorption peaks in THz spectra valuable for crystal quality evaluation of middle molecular weight pharmaceuticals," *J. Infr., Millim., THz Waves*, vol. 39, no. 9, pp. 828–839, Sep. 2018, doi: 10.1007/s10762-018-0494-2.

[6] A. Duhant, M. Triki, and O. Strauss, "Terahertz differential computed tomography: A relevant nondestructive inspection application," *J. Infr., Millim., THz Waves*, vol. 40, no. 2, pp. 178–199, Feb. 2019, doi: 10.1007/s10762-018-0564-5.

[7] M. Nagel, M. Först, and H. Kurz, "THz biosensing devices: Fundamentals and technology," *J. Phys., Condens. Matter*, vol. 18, no. 18, pp. S601–S618, May 2006, doi: 10.1088/0953-8984/18/18/S07.

[8] T. Kiwa, Y. Kondo, Y. Minami, I. Kawayama, M. Tonouchi, and K. Tsukada, "Terahertz chemical microscope for label-free detection of protein complex," *Appl. Phys. Lett.*, vol. 96, no. 21, May 2010, Art. no. 211114, doi: 10.1063/1.3441408.

[9] F. Taleb, I. Al-Naib, and M. Koch, "Free-standing complementary asymmetric metasurface for terahertz sensing applications," *Sensors*, vol. 20, no. 8, p. 2265, Apr. 2020, doi: 10.3390/s20082265.

[10] T. Nagatsuma, G. Ducournau, and C. C. Renaud, "Advances in terahertz communications accelerated by photonics," *Nature Photon.*, vol. 10, no. 6, pp. 371–379, Jun. 2016, doi: 10.1038/nphoton.2016.65.

[11] D. L. Renaud and J. F. Federici, "Terahertz attenuation in snow and sleet," *J. Infr., Millim., THz Waves*, vol. 40, no. 8, pp. 868–877, Aug. 2019, doi: 10.1007/s10762-019-00607-y.

[12] J. Ma, R. Shrestha, W. Zhang, L. Moeller, and D. M. Mittleman, "Terahertz wireless links using diffuse scattering from rough surfaces," *IEEE Trans. THz Sci. Technol.*, vol. 9, no. 5, pp. 463–470, Sep. 2019, doi: 10.1109/TTHZ.2019.2933166.

[13] C. Liu, J. Ye, and Y. Zhang, "Thermally tunable THz filter made of semiconductors," *Opt. Commun.*, vol. 283, no. 6, pp. 865–868, Mar. 2010, doi: 10.1016/j.optcom.2009.11.019.

[14] C. Jansen, S. Wietzke, V. Astley, D. M. Mittleman, and M. Koch, "Mechanically flexible polymeric compound one-dimensional photonic crystals for terahertz frequencies," *Appl. Phys. Lett.*, vol. 96, no. 11, Mar. 2010, Art. no. 111108, doi: 10.1063/1.3341309.

[15] S. F. Busch, M. Weidenbach, J. C. Balzer, and M. Koch, "THz optics 3D printed with TOPAS," *J. Infr., Millim., THz Waves*, vol. 37, no. 4, pp. 303–307, Apr. 2016, doi: 10.1007/s10762-015-0236-7.

[16] C.-J. Lin, Y.-T. Li, C.-F. Hsieh, R.-P. Pan, and C.-L. Pan, "Manipulating terahertz wave by a magnetically tunable liquid crystal phase grating," *Opt. Exp.*, vol. 16, no. 5, p. 2995, 2008, doi: 10.1364/OE.16.002995.

[17] D. W. Vogt and R. Leonhardt, "3D-printed broadband dielectric tube terahertz waveguide with anti-reflection structure," *J. Infr., Millim., THz Waves*, vol. 37, no. 11, pp. 1086–1095, Nov. 2016, doi: 10.1007/s10762-016-0296-3.

[18] J. Ma, M. Weidenbach, R. Guo, M. Koch, and D. M. Mittleman, "Communications with THz waves: Switching data between two waveguides," *J. Infr., Millim., THz Waves*, vol. 38, no. 11, pp. 1316–1320, Nov. 2017, doi: 10.1007/s10762-017-0428-4.

[19] T. Niu, W. Withayachumnankul, A. Upadhyay, P. Gutruf, D. Abbott, M. Bhaskaran, S. Sriram, and C. Fumeaux, "Terahertz reflectarray as a polarizing beam splitter," *Opt. Exp.*, vol. 22, no. 13, p. 16148, Jun. 2014, doi: 10.1364/OE.22.016148.
[20] J. Masson and G. Gallot, "Terahertz achromatic quarter-wave plate Jean-Baptiste," *Opt. Lett.*, vol. 31, no. 2, pp. 265–267, 2006, doi: 10.1002/cncr.21761.
[21] J. Ornik, L. Gomell, S. F. Busch, M. Hermans, and M. Koch, "High quality terahertz glass wave plates," *Opt. Exp.*, vol. 26, no. 25, p. 32631, Dec. 2018, doi: 10.1364/OE.26.032631.
[22] S. Pandey, B. Gupta, and A. Nahata, "Terahertz plasmonic waveguides created via 3D printing," *Opt. Exp.*, vol. 21, no. 21, p. 24422, Oct. 2013, doi: 10.1364/OE.21.024422.
[23] H. Xin and M. Liang, "3-D-printed microwave and THz devices using polymer jetting techniques," *Proc. IEEE*, vol. 105, no. 4, pp. 737–755, Apr. 2017, doi: 10.1109/JPROC.2016.2621118.
[24] D. W. Vogt, J. Anthony, and R. Leonhardt, "Metallic and 3D-printed dielectric helical terahertz waveguides," *Opt. Exp.*, vol. 23, no. 26, p. 33359, Dec. 2015, doi: 10.1364/OE.23.033359.
[25] D. Jahn, M. Weidenbach, J. Lehr, L. Becker, F. Beltrán-Mejía, S. F. Busch, J. C. Balzer, and M. Koch, "3D printed terahertz focusing grating couplers," *J. Infr., Millim., THz Waves*, vol. 38, no. 6, pp. 708–716, Jun. 2017, doi: 10.1007/s10762-017-0370-5.
[26] W. J. Otter and S. Lucyszyn, "Hybrid 3-D-printing technology for tunable THz applications," *Proc. IEEE*, vol. 105, no. 4, pp. 756–767, Apr. 2017, doi: 10.1109/JPROC.2016.2629958.
[27] S. F. Busch, M. Weidenbach, M. Fey, F. Schäfer, T. Probst, and M. Koch, "Optical properties of 3D printable plastics in the THz regime and their application for 3D printed THz optics," *J. Infr., Millim., THz Waves*, vol. 35, no. 12, pp. 993–997, Dec. 2014, doi: 10.1007/s10762-014-0113-9.
[28] W. D. Furlan, V. Ferrando, J. A. Monsoriu, P. Zagrajek, E. Czerwińska, and M. Szustakowski, "3D printed diffractive terahertz lenses," *Opt. Lett.*, vol. 41, no. 8, p. 1748, Apr. 2016, doi: 10.1364/ol.41.001748.
[29] M. Ortiz-Martinez, E. Castro-Camus, and A. I. Hernandez-Serrano, "Guided-mode filters for terahertz frequencies fabricated by 3D printing," *J. Infr., Millim., THz Waves*, vol. 40, no. 7, pp. 731–737, Jul. 2019, doi: 10.1007/s10762-019-00602-3.
[30] E. Castro-Camus, M. Koch, and A. I. Hernandez-Serrano, "Additive manufacture of photonic components for the terahertz band," *J. Appl. Phys.*, vol. 127, no. 21, Jun. 2020, Art. no. 210901, doi: 10.1063/1.5140270.
[31] K. Z. Rajab, M. Naftaly, E. H. Linfield, J. C. Nino, D. Arenas, D. Tanner, R. Mittra, and M. Lanagan, "Broadband dielectric characterization of aluminum oxide (Al_2O_3)," *J. Microelectron. Electron. Packag.*, vol. 5, no. 1, pp. 2–7, Jan. 2008, doi: 10.4071/1551-4897-5.1.1.
[32] A. K. Klein, J. Hammler, C. Balocco, and A. J. Gallant, "Machinable ceramic for high performance and compact THz optical components," *Opt. Mater. Exp.*, vol. 8, no. 7, p. 1968, Jul. 2018, doi: 10.1364/OME.8.001968.
[33] F. Rutz, N. Krumbholz, L. Micele, G. de Portu, D. M. Mittleman, and M. Koch, "Improved dielectric mirrors for the THz frequency range," *Proc. SPIE*, vol. 6194, Apr. 2006, Art. no. 61940K, doi: 10.1117/12.661610.
[34] Y. Kim, M. Yi, B. G. Kim, and J. Ahn, "Investigation of THz birefringence measurement and calculation in Al_2O_3 and $LiNbO_3$," *Appl. Opt.*, vol. 50, no. 18, p. 2906, Jun. 2011, doi: 10.1364/AO.50.002906.
[35] Z. Chen, Z. Li, J. Li, C. Liu, C. Lao, Y. Fu, C. Liu, Y. Li, P. Wang, and Y. He, "3D printing of ceramics: A review," *J. Eur. Ceram. Soc.*, vol. 39, no. 4, pp. 661–687, Apr. 2019, doi: 10.1016/j.jeurceramsoc.2018.11.013.
[36] M. Schwentenwein, P. Schneider, and J. Homa, "Lithography-based ceramic manufacturing: A novel technique for additive manufacturing of high-performance ceramics," *Adv. Sci. Technol.*, vol. 88, pp. 60–64, Oct. 2014, doi: 10.4028/www.scientific.net/ast.88.60.
[37] M. Schwentenwein and J. Homa, "Additive manufacturing of dense alumina ceramics," *Int. J. Appl. Ceram. Technol.*, vol. 12, no. 1, pp. 1–7, Jan. 2015, doi: 10.1111/ijac.12319.
[38] W. Harrer, M. Schwentenwein, T. Lube, and R. Danzer, "Fractography of zirconia-specimens made using additive manufacturing (LCM) technology," *J. Eur. Ceram. Soc.*, vol. 37, no. 14, pp. 4331–4338, Nov. 2017, doi: 10.1016/j.jeurceramsoc.2017.03.018.
[39] A. Jimenez-Saez, M. Schubler, C. Krause, D. Pandel, K. Rezer, G. V. Bogel, N. Benson, and R. Jakoby, "3D printed alumina for low-loss millimeter wave components," *IEEE Access*, vol. 7, pp. 40719–40724, 2019, doi: 10.1109/ACCESS.2019.2906034.
[40] A. Jimenez-Saez, M. Schusler, D. Pandel, N. Benson, and R. Jakoby, "3D printed 90 GHz frequency-coded chipless wireless RFID tag," in *Proc. IEEE MTT-S Int. Microw. Workshop Ser. Adv. Mater. Processes RF THz Appl. (IMWS-AMP)*, Jul. 2019, pp. 4–6, doi: 10.1109/IMWS-AMP.2019.8880140.
[41] A. Jiménez-Sáez, A. Alhaj-Abbas, M. Schüßler, A. Abuelhaija, M. El-Absi, M. Sakaki, L. Samfaß, N. Benson, M. Hoffmann, R. Jakoby, T. Kaiser, and K. Solbach, "Frequency-coded mm-wave tags for self-localization system using dielectric resonators," *J. Infr., Millim., THz Waves*, vol. 41, no. 8, pp. 908–925, Aug. 2020, doi: 10.1007/s10762-020-00707-0.
[42] A. M. Abyzov, "Aluminum oxide and alumina ceramics (review). Part 1. Properties of Al_2O_3 and commercial production of dispersed Al_2O_3," *Refractories Ind. Ceram.*, vol. 60, no. 1, pp. 24–32, May 2019, doi: 10.1007/s11148-019-00304-2.
[43] *Lithoz: 3D-Druck für Keramik*. Accessed: Jul. 10, 2020 [Online]. Available: https://www.lithoz.com/
[44] N. Vieweg, F. Rettich, A. Deninger, H. Roehle, R. Dietz, T. Göbel, and M. Schell, "Terahertz-time domain spectrometer with 90 dB peak dynamic range," *J. Infr., Millim., THz Waves*, vol. 35, no. 10, pp. 823–832, Oct. 2014, doi: 10.1007/s10762-014-0085-9.
[45] R. Wilk, I. Pupeza, R. Cernat, and M. Koch, "Highly accurate THz time-domain spectroscopy of multilayer structures," *IEEE J. Sel. Topics Quantum Electron.*, vol. 14, no. 2, pp. 392–398, Apr. 2008, doi: 10.1109/JSTQE.2007.910981.
[46] M. Scheller, C. Jansen, and M. Koch, "Analyzing sub-100-μm samples with transmission terahertz time domain spectroscopy," *Opt. Commun.*, vol. 282, no. 7, pp. 1304–1306, Apr. 2009, doi: 10.1016/j.optcom.2008.12.061.
[47] B. Zhang and Y. Gong, "Achromatic terahertz quarter waveplate based on silicon grating," *Opt. Exp.*, vol. 23, no. 11, p. 14897, Jun. 2015, doi: 10.1364/OE.23.014897.
[48] M. Scheller, C. Jördens, and M. Koch, "Terahertz form birefringence," *Opt. Exp.*, vol. 18, no. 10, p. 10137, May 2010, doi: 10.1364/OE.18.010137.

JAN ORNIK received the B.Sc. and M.Sc. degrees in physics from the Faculty of Natural Science and Mathematics, University of Maribor, Slovenia, in 2013 and 2016, respectively. He is currently pursuing the Ph.D. degree in the field of terahertz spectroscopy with Philipps-University Marburg, Germany, under the supervision of Prof. Martin Koch.

MASOUD SAKAKI received the Ph.D. degree in materials science and engineering in 2010. His main expertise is synthesis, characterization, and sintering of ceramic compounds via different routes. He was an Assistant Professor with Malayer University, Iran, from 2010 to 2014, and a Postdoctoral Researcher with Kochi University, Japan, from 2014 to 2019. He is currently a Postdoctoral Researcher with Duisburg-Essen University. His research is focused on the additive manufacturing of ceramics for THz applications.

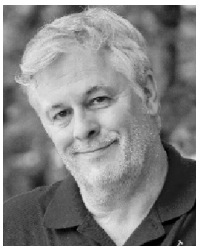

MARTIN KOCH received the Diploma and Ph.D. degrees in physics from Philipps-Universität Marburg, Marburg, Germany, in 1991 and 1995, respectively.

He was a Postdoctoral Fellow with Bell Labs/Lucent Technologies, Holmdel, NJ, USA, from 1995 to 1996. From 1996 to 1998, he was with the Photonics and Optoelectronics Group, University of Munich, Munich, Germany. Since 1998, he has been an Associate Professor with the Department of Electrical Engineering, Technische Universität Braunschweig, Brunswick, Germany. In 2003, he spent a three-month sabbatical at the University of California at Santa Barbara, Santa Barbara. Since 2009, he has been a Professor of experimental semiconductor physics with Philipps-Universität Marburg.

Prof. Koch was a recipient of the Kaiser-Friedrich Research Prize in 2003 and the IPB Patent Award in 2009. In 2019, he received the Exceptional Service Award from the IRMMW-THz Society. He is the Editor-in-Chief of the *Journal of Infrared, Millimeter, and Terahertz Waves*.

JAN C. BALZER received the Dipl.-Ing. degree (Hons.) in telecommunications from the Dortmund University of Applied Sciences and Arts, Germany, in 2008, the M.Sc. degree in electrical engineering and information technology and the Ph.D. degree in electrical engineering from Ruhr-Universität Bochum, Germany, in 2010 and 2014, respectively. His Ph.D. thesis was on ultrafast semiconductor lasers.

In 2015, he joined as a Postdoctoral Research Fellow with the Experimental Physics Group, Philipp-Universität Marburg, with his main research interests in THz technology and its applications. Since 2017, he has been an Assistant Professor for THz systems with the Faculty of Engineering, University of Duisburg-Essen, where he combines his knowledge of ultrafast semiconductor lasers with his expertise in system building of THz spectrometers.

NIELS BENSON (Member, IEEE) received the Dipl.-Ing. degree in electrical engineering from the University of Stuttgart, in 2004, and the Dr.-Ing. degree in materials science from the Technische Universität Darmstadt, in 2009. Since 2008, he was a Senior Scientist for polymer vision on rollable active matrix displays. In 2010, he joined the University of Duisburg-Essen as a Research Group Leader on thin film photovoltaics and electronics. In 2018, he was appointed a W1-Professor with the University of Duisburg-Essen on printable materials for signal processing systems. His current research interests include charge carrier transport in disordered semiconductor NIELSBENSON.pdfsystems, passive chipless RFID systems, and additive manufactured ceramic components for sub-mm and mm-wave signal processing applications.